Innovative Food Science and Emerging Technologies 52 (2019) 145–157

Contents lists available at ScienceDirect

Innovative Food Science and Emerging Technologies

journal homepage: www.elsevier.com/locate/ifset

Characterization of CO_2 laser browning of dough

Jonathan David Blutinger[a,*], Yorán Meijers[a,b], Peter Yichen Chen[a], Changxi Zheng[a], Eitan Grinspun[a], Hod Lipson[a]

[a] Columbia University, 500 W 120 St., New York, NY 10027, United States of America
[b] Wageningen University, 6708 PB Wageningen, Netherlands

ARTICLE INFO

Keywords:
CO_2 laser
Dough
Browning
Flux
Starch gelatinization
Food layered manufacture

ABSTRACT

We study the application of laser-heating technology to browning dough, due to its potential for high-resolution spatial and surface color control. An important component of this process is the identification of how laser parameters affect browning and baking and whether desirable results can be achieved. In this study, we analyze the performance of a carbon dioxide (CO_2) mid-infrared laser (operating at 10.6 μm wavelength) during the browning of dough. Dough samples—consisting of flour and water—were exposed to the infrared laser at different laser power, beam diameter, and sample exposure time. At a laser energy flux of 0.32 MW m^{-2} (beam diameter of 5.7 mm) and sample exposure time of 180 s we observe a maximum thermal penetration of 0.77 mm and satisfactory dough browning. These results suggest that a CO_2 laser is ideal for browning thin goods as well as for food layered manufacture.

Industrial relevance: A CO_2 laser that operates at a wavelength of 10.6 μm (IR) was used as an alternative method for browning dough. The high-power flux of the laser and the high energy absorption of food at this wavelength allow for rapid surface browning; however, the high absorption limits thermal penetration depth. Nevertheless, accuracy of the laser beam enables high resolution spatial and thermal control of the non-enzymatic browning process. This high precision cooking makes laser-browning particularly ideal for food layered manufacture (FLM), a food processing technique that has gained increased attention in recent years. Using FLM, one can adjust the printed layer height to match cooking penetration depth. As a digital manufacturing technology, laser-browning could also enable manufacture of highly complex and customized food geometries and textures.

1. Introduction

Lasers offer a relatively unexplored food processing technique useful for precision cooking. Potential applications range from browning food in a microwave to broiling thin layers of food using software-driven patterns. One particular application of laser cooking is its use in conjunction with Food Layered Manufacture (FLM). FLM is an application of additive manufacturing technology that utilizes food as a material to print three-dimensional (3D) food products.

Food printing, first demonstrated by Periard et al. (2007), has become a growing trend (Lipson & Kurman, 2013; Sun et al., 2015; Wegrzyn, Golding, & Archer, 2012). Due to the thin layer deposition of food in an FLM application and the ability to print multi-ingredient food products (Hertafeld et al., 2018), precise heat delivery is needed (Zoran & Coelho, 2011) to tune heating parameters for each food ingredient. While laser technology is used extensively in medical (Gordon, 2000; Wheeland, 1995) and industrial applications (Kaplan, 1994), their ability to provide targeted and repeatable energy make them ideal for use in some areas of food cooking (Blutinger et al., 2018). The specific characteristics of lasers for food processing include their ability to provide uniform heating, repeatable and precise control of energy delivery, resolution of spatial placement of the energy, and precise localized heating (Singh, 2013).

We have previously explored the use of lasers to bake dough (Blutinger et al., 2018). We parameterized the use of a blue laser to bake dough and found that it can provide the necessary heat to gelatinize starch, yet it lacks the ability to effectively brown the surface of dough (Blutinger et al., 2018). Aside from this investigation into laser-heating, other published research regarding laser cooking is very limited. Lasers are applied in additive manufacturing for selective laser sintering (SLS) of edible objects, but the technique is limited to a specific range of food powders (Diaz et al., 2014). Fukuchi, Jo, Tomiyama, and Takao (2012) reports the use of a CO_2 laser cutter to selectively cook the fat portion of bacon while leaving the meat untouched. Other

* Corresponding author.
E-mail addresses: jdb2202@columbia.edu (J.D. Blutinger), cyc@cs.columbia.edu (P.Y. Chen), cxz@cs.columbia.edu (C. Zheng), eitan@cs.columbia.edu (E. Grinspun), hod.lipson@columbia.edu (H. Lipson).

https://doi.org/10.1016/j.ifset.2018.11.013
Received 10 April 2018; Received in revised form 30 October 2018; Accepted 28 November 2018
Available online 29 November 2018
1466-8564/

researchers have used a CO_2 laser for the improvement of food quality, specifically for clarification and antimicrobial irradiation (Panchev, Kirtchev, & Dimitrov, 2011). Additionally, several patents regarding laser cooking exist. Muchnik (2008) reported the use of a CO_2 laser to rapidly cook food, Singh (2013) used several types of lasers to prepare foods and Gracia and Sepulveda (2015) combined lasers and electromagnetic waves in the cooking chamber of a 3D food printer. Regrettably, these patents do not characterize optimal laser heating parameters, thus further studies are required to advance understanding of laser cooking.

Dough color can suggest certain textural properties such as firmness, stiffness, hardness, and—most importantly—serve as an indicator of quality (Abdullah, 2008; Ahrné et al., 2007). The driving force behind these structural changes in dough is temperature (Ploteau, Glouannec, Nicolas, & Magueresse, 2015). Formation of color by heating can be attributed to non-enzymatic browning processes (i.e., Maillard reaction and caramelization) (Purlis, 2010). Conventional ovens do not lend themselves well to controlling the browning process since heat distribution is uniform with no high-fidelity heating capabilities (Datta & Rakesh, 2013). As such, this paper aims to explore the extent of browning development in laser-heated dough.

Complete starch gelatinization is another important indicator of dough quality, which is used to qualify sensory acceptability (Purlis, 2012). Degree of starch gelatinization can be used as an indication of product digestibility and nutritional content (Wang & Copeland, 2013). The temperature and moisture dependence of the starch gelatinization process has been studied extensively (Lineback & Wongsrikasem, 1980; Mondal & Datta, 2008; Olkku & Rha, 1978; Wang & Copeland, 2013; Zanoni, Peri, & Bruno, 1995). Notably, it was found that complete starch gelatinization is achieved one the dough core reaches 95 °C (Zanoni et al., 1995). Due to the size of wheat starch granules (Olkku & Rha, 1978), scanning electron microscopy (SEM) can be used to capture the dough microstructure and assess for the completion of the gelatinization process (Almeida & Chang, 2013; Miller, Derby, & Trimbo, 1973). SEM has been used to characterize changes in potato starch granules (Huang et al., 1990) and assess the quality of laser-baked dough (Blutinger et al., 2018).

Heating characteristics of lasers are very much dependent on the light's operating wavelength. Longwave infrared (IR) light provides faster heating rates (Westerberg, 1998) while shorter wavelength radiation provides deeper heat penetration (Blutinger et al., 2018; Dessev, Jury, & Le-Bail, 2011; Lentz et al., 1995; Skjöldebrand & Andersson, 1989). The CO_2 laser (10.6 μm wavelength) used in this study falls in the mid-infrared (MIR) region of the electromagnetic spectrum (based on ISO 20473) and shows high absorbance by organic materials (Baranov et al., 2005). While the radiation depth of the MIR energy only reaches a few microns (Salagnac, Glouannec, & Lecharpentier, 2004), the energy is transferred via conduction to the inner part of the food being heated (Lentz et al., 1995). This laser's high-resolution (millimeter scale) heating capabilities make it ideal for various food applications, including in situ food processing for FLM and the addition of grill marks on foods (Griesbach et al., 2004).

We investigate the ability of a CO_2 laser (Fig. 1) to effectively brown dough. Dough consisting of flour and water was prepared as a model food system to develop an understanding of the parameters of a CO_2 laser. Two approaches were taken to observe browning, thermal penetration, and the general appearance of the food product: 1) the dough was exposed to different amounts of total laser energy and 2) a constant total laser energy was maintained to observe the effects of varying laser intensity (or beam flux, measured in $W\,m^{-2}$). Additional tests conducted on the dough samples include measurement of weight loss after heating, measurement of temperature during the laser-heating process, imaging to assess degree of browning, and SEM-imaging to examine microstructure and degree of starch gelatinization.

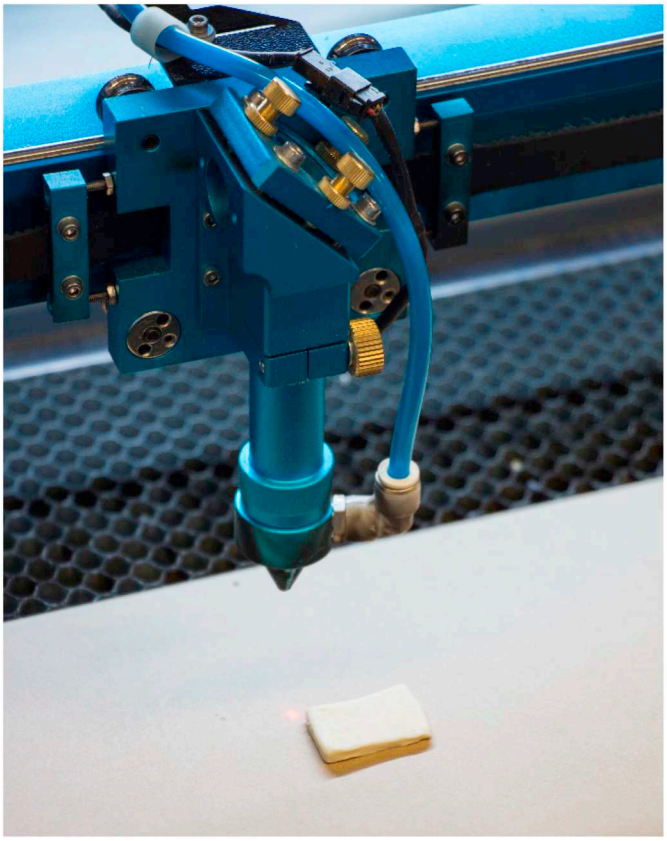

Fig. 1. Experimental setup showing uncooked dough sample prior to CO_2 laser exposure. The laser head (blue nozzle) is mounted to a track that allows it to move in 2D Cartesian space. The laser bed (honeycomb mesh) moves in the z-direction, thereby affecting the laser energy flux that interacts with the dough sample.

2. Materials and methods

2.1. Dough sample preparation

Commercial all-purpose flour (Heckers, Kansas City, USA) was acquired for this study. According to the manufacturer, 100 g of flour contains 73 g of carbohydrate and 10 g of protein. To prepare the dough, 200 g of flour was mixed with 120 g of tap water for 2 min at low speed in a food processor (FP-8FR series, Cuisinart, East Windsor, USA) at ambient temperature (23 °C). The recipe did not include yeast to prevent fermentation and expansion of the dough during further processing. After mixing, the dough was left to rest for 15 min and stored at 4 °C to prevent reactions from taking place within the dough. The dough was divided into small pieces and laminated with a roller until a thickness of 2 mm (± 0.1 mm) was achieved. Finally, the dough sheet was cut into squares of side length 30 mm.

2.2. Laser apparatus

A CO_2 laser cutter and engraver (Nova 35, Thunder Laser Equipment Co., Ltd., Dongguan, China) was used in this study, operating at the infrared wavelength of 10.6 μm with a maximum allowable power of 80 W (Fig. 1). RDWorks V.8 software was used to set laser parameters. Scan mode (x-swing) was applied for all heating purposes, with a 0.1 mm interval between passes. The software allowed for a laser speed of up to 1000 $mm\,s^{-1}$ and laser power of 10 to 70% (8 to 56 W).

The manufacturer states that the power consumption for the 80 W laser is 1400 W (yielding a 6% efficiency).

2.3. Image acquisition of dough samples

A controlled environment was maintained for repeatable image capture. The samples were placed in a white ceramic bowl with one light source from directly above the bowl. The bowl was white to reflect the light and create a uniform lighting condition. The camera, mounted to a tripod, was angled downward directly above the bowl opening, giving a top view of the browned samples. This setup was maintained for the duration of the experiments.

All of the photos were taken using a digital single-lens reflex camera (EOS Rebel T5i, Canon, Tokyo, Japan). The images were taken in uncompressed form as a "Canon Raw Version 2" to allow for the highest resolution. Post-processing of the images involved color balancing all of the photos with a white color swatch, which was placed into the environment. Adobe Photoshop CS6 was used to correct the images to a known color value. The $L^*a^*b^*$ color model was used for the symbolic regression in Section 3.2.3 since it has the largest gamut of colors among all the color models (i.e., *RGB*, *CMYK*, *HSV*) (Yam & Papadakis, 2004). Cropping and white color adjustment were the only post-processing performed on the original images.

2.4. Determination of laser beam divergence

The Nova 35 laser uses a lens to focus the beam. This particular laser has a focus distance of 4.5 mm, which is where the beam waist occurs (beam diameter = 0.1 mm) and energy flux is at a maximum. The manufacturer of the laser does not have documentation regarding the beam divergence, hence one must calculate the half-angle (measure of divergence) experimentally. Height in the z coordinate is used to refer to the distance from the laser head to the surface of the sample (Fig. 3). Further analysis was needed in order to determine the divergence of the beam as a function of z.

To assess the beam divergence, lines were etched onto a piece of acrylic at constant speed and power at various heights. Following these tests, high-quality photos were taken of the etched lines using a macro lens (EF 100 mm f/2.8 Macro USM Lens, Canon, Tokyo, Japan). In Photoshop, the width of the heat-affected zone (HAZ) on the acrylic was measured on the enlarged images (Fig. 2). HAZ refers to the area on the acrylic (or dough) that was affected by the heat of the laser beam, the extent of which is also affected by the speed of the moving laser.

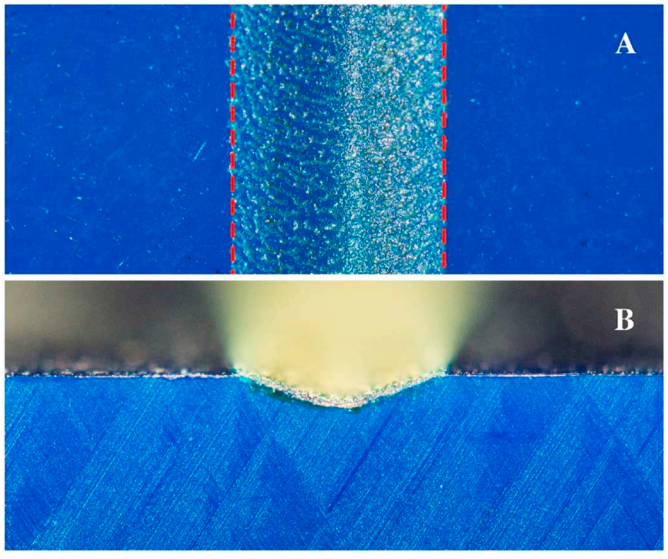

Fig. 2. Acrylic exposed to the CO_2 laser beam. The HAZ on the acrylic lies between the red dashed lines. A) Top view of HAZ. B) Side view of HAZ.

2.5. Calculating variables that affect dough browning

The main variables that affected the degree of dough browning from continued laser exposure include total laser energy per beam area (e, J m^{-2}), laser beam flux (f, W m^{-2}), point exposure time (p, s), and variance of laser energy supplied to each dough sample (v). Laser speed (s, m s^{-1}), beam diameter (d, m), laser power (P, W), sample exposure time (t, s), dough sample side length (w, m), and gap between laser scan lines (g, m) are the main variables used to calculate these four derived units.

Laser flux (f) was calculated using Eq. (1), where power is divided by the total area of the beam, yielding the appropriate units of power per area (W m^{-2}).

$$f = \frac{4P}{\pi d^2} \tag{1}$$

To calculate the total laser energy supplied per beam area to the dough sample during a trial, Eq. (2) was used.

$$e = \frac{fw^2}{gs} \tag{2}$$

Point exposure time (p) is another derived unit that is calculated using the following method (Eq. (3)):

$$p = \frac{\pi d^2 t}{4w^2}. \tag{3}$$

Finally, variance of laser energy supplied to the dough was calculated used MATLAB, computer software optimal for data processing. A custom simulation was generated to model the laser beam (assumed to be Gaussian) as it scanned a 30 mm square dough sample. The dough was split into voxels of square length 0.1 mm and energy over time was recorded for each voxel on the dough surface as the laser performed an x-swing raster scanning pattern. Energy variance over time was recorded for the square voxel in the center of the dough and the variance of laser energy over time was calculated for the simulated time series.

2.6. Measuring weight loss in the laser-heated dough

Weight loss was measured immediately after sample preparation by calculating the difference between the weight before and after laser processing. This value was converted into a percentage by dividing the change in mass by the preheated mass of the dough in order to provide a more comparable unit of measure. Measurements were performed in duplicate and error bars indicate standard error of the mean, except where noted.

2.7. Measuring thermal penetration depth in laser-heated dough

After laser heating, the samples were cut in half. Depth of heat penetration was determined by a visual assessment of the transition of dough into crumb and crust. A digital caliper (0.02 mm accuracy) was used to measure the depth of heat penetration. Due to the resolution of the measuring tool, the smallest thermal penetration depth was assumed to be 0.1 mm. The measurements were performed in duplicate and error bars indicate standard error except where noted.

2.8. Measuring temperature within the dough

To measure the temperature inside the dough at different distances from the surface, two Leaton 4-Channel K-Type Digital Thermometer Thermocouple Sensors were used, each with four K-thermocouples (at 1 °C accuracy); allowing for eight points of temperature data. The thermocouples were inserted into a raw dough sample at increasing

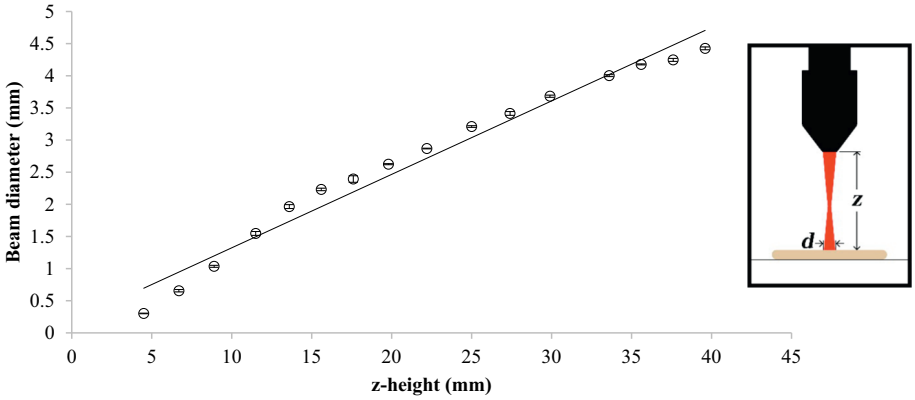

Fig. 3. Beam diameter as a function of *z*-height. The error bars indicate standard error (SE) (n = 3). There is a direct linear relationship between *z*-height (*z*) and beam diameter (d). Inset schematic shows how *z* and d are measured. From top to bottom: in black is the laser head, in red is the laser beam, and in tan is the dough sample.

depths below the surface. Each thermocouple was placed at steps of 0.25 mm from the surface; the deepest thermocouple was at 2 mm from the surface. The measurements were performed in duplicate and error bars indicate standard error except where noted.

2.9. Analyzing dough microstructure via SEM

The microstructure of the dough and the laser-heated samples was examined under an SEM (Sigma VP, Zeiss, Oberkochen, Germany), under the following conditions: high vacuum ($< 2 \cdot 10^{-5}$ Pa), a working distance of 3.5 mm, and an acceleration voltage of 5 kV. Prior to SEM analysis, samples were oven-dried at 50 °C overnight and sputter-coated with gold.

3. Results and discussion

3.1. Calculating laser beam divergence

The laser uses a lens to focus the beam. The manufacturer of the laser reports that the laser is focused at a distance of 4.5 mm. To calculate the divergence of the laser beam, a piece of acrylic was exposed to the laser beam (Fig. 2) at different *z*-heights. The beam diameter was determined by image analysis of the heat-affected area on the piece of acrylic. Three measurements were taken for each beam diameter. The mean and standard deviation were calculated and a linear regression was performed on this data (Fig. 3). It was assumed that the width of the HAZ is equivalent to the full diameter of the infrared beam, and that the divergence angle is constant (Steen & Mazumder, 2010). Under these assumptions, the following relationship was found (with $R^2 = 0.97$):

$$\boldsymbol{d = 0.1143z + 0.1804} \quad (4)$$

where *d* is the beam diameter (mm) and *z* is the height of the laser (mm), measured as shown in the diagram inset in Fig. 3.

Eq. (4) was used to calculate the beam diameter for different *z* distances. The energy profile can be modeled as a normal distribution (Steen & Mazumder, 2010) since the beam is assumed to be Gaussian. Since the beam power remains constant during the tests, only the intensity profile will change as a result of changing the beam diameter (i.e. the area under the intensity profile curve will remain constant). To accurately plot the beam intensity profiles (Fig. 4), the standard deviations of the Gaussian curves were set to 1/6th of the beam diameter. Fig. 4 is a 2D representation of the variance in laser power that is supplied to a dough voxel on the surface of the sample each time the center of the beam passes over. It becomes evident that the larger the beam diameter, the more diffuse the energy profile of the beam, and the closer the beam starts to simulate a uniform heating environment. There is a tradeoff between resolution and uniformity that becomes apparent through the analysis of the beam intensity.

3.2. Laser browning of dough samples

3.2.1. Effect of laser flux and exposure time on dough browning

An experiment was designed to develop an understanding of the effect of laser intensity ($W\,m^{-2}$) on dough surface browning. At fixed power (8 W) and fixed exposure time (45 s), the energy flux of the laser beam was varied (by changing *z*). Throughout these tests, the CO_2 laser followed an x-swing raster scanning pattern over the entire sample followed by a y-swing scanning pattern for the left half of each dough sample. Exposing half of the sample to a second laser pass made it possible to compare how repeated laser exposure affects dough browning.

Beam flux has a strong effect on the appearance of the laser-heated dough (Fig. 5). A visible change in browning and water evaporation becomes apparent by changing the flux supplied to the dough. In the first four tiles (A through D) of Fig. 5, it can be seen that the second pass of the laser on the dough causes a deepening effect. The deepening effect suggests that the heat flux supplied to the surface caused all water

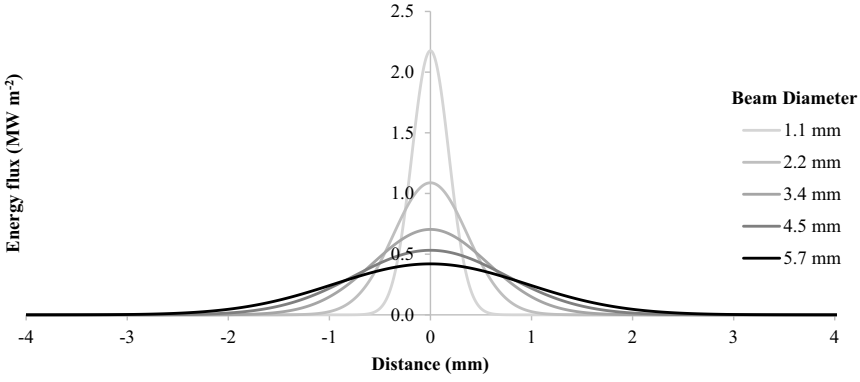

Fig. 4. 2D representation of laser intensity profiles at different beam diameters. The five beam diameters correspond to the beam fluxes used in the experiments. The area under each curve represents the power supplied by the beam, which is constant at 8 W. A more diffuse beam will have a lower peak while a more intense beam will have a high peak.

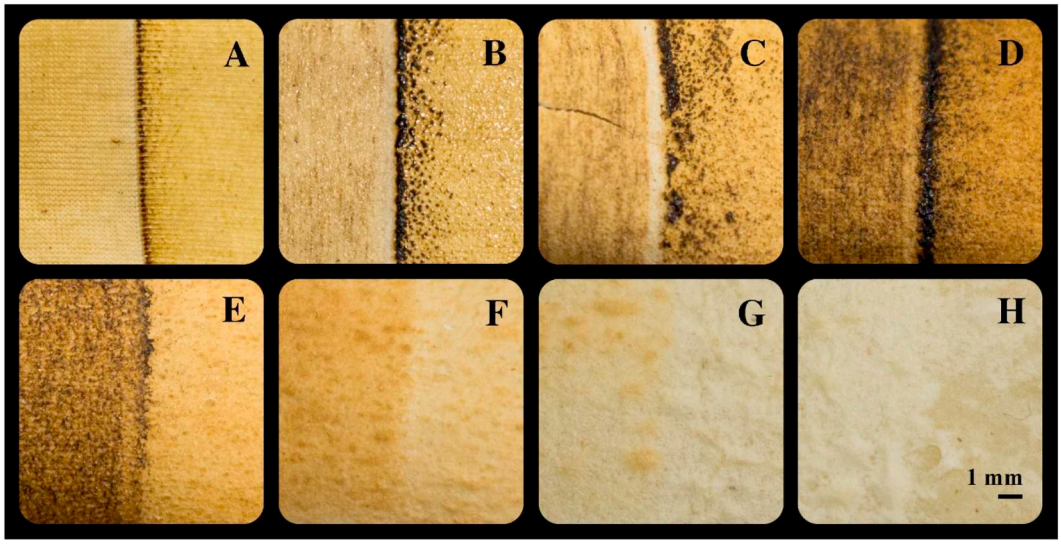

Fig. 5. Dough exposed to a laser beam (8 W, sample exposure time = 45 s) at decreasing beam flux. A) 21 MW m^{-2}, B) 6.4 MW m^{-2}, C) 3.0 MW m^{-2}, D) 1.8 MW m^{-2}, E) 1.1 MW m^{-2}, F) 0.8 MW m^{-2}, G) 0.6 MW m^{-2}, H) 0.5 MW m^{-2}. The right-hand portion of each sample has been cooked once, while the left-hand portion has been cooked twice. Optimal browning starts to occur in sample E.

to rapidly evaporate. The dough dries out before browning reactions can take place and turns into a powder. Further increase in the beam diameter however will decrease the heat flux, allowing more time for browning reactions to take place, since water evaporates less rapidly. At a beam flux of 1.1 MW m^{-2} (E, Fig. 5), no deepening effect can be observed and the second pass of the laser increases browning. As the optical intensity decreases further (E through H, Fig. 5), laser flux isn't sufficient to increase the dough surface temperature fast enough to allow water to evaporate and cause browning reactions.

Singh (2013) also reported a clear relationship between laser beam diameter and applicable cooking threshold. Increasing beam diameter will decrease laser resolution and laser flux variance. A low variance in the supplied energy will resemble a more uniform conventional heating process, such as a convection oven. Minimum tunable laser power for these experiments was 8 W, resulting in a heat flux of approximately 8.5 MW m^{-2} at a beam diameter of 1.1 mm and 0.32 MW m^{-2} at a beam diameter of 5.7 mm. These values are high compared to infrared baking, where heat flux values are closer to 1050 and 5500 W m^{-2} (Dessev et al., 2011). This difference in energy flux can be accounted for with a difference in exposure time. Infrared baking uniformly exposes the product to heat for the entire heating process, while laser heating exposes dough to the beam spot for a limited duration, resulting in "pulsed heating".

These results indicate that there is a narrow range of laser energy fluxes suitable for browning. In the experiments that follow (Fig. 6), laser energy flux and sample exposure time were varied by adjusting *z*-height and laser speed, respectively. Overexposure to infrared radiation impaired quality of dough browning (Rastogi, 2015). At high optical intensity (beam diameter of 1.1 mm), the surface of the sample either lacks browning development (e.g. exposure time 36 and 45 s) or is covered by a layer of powder due to dough vaporization. Samples laser heated at high exposure times produced more powder because moisture evaporation was too fast for browning reactions to occur.

High power density can significantly affect the usual baking behavior of dough (Salagnac et al., 2004). This altered baking behavior can be observed at a beam flux of 2.03 MW m^{-2} and an exposure time of 180 s (Fig. 6), where a great deal of browning occurs. At this energy flux (2.03 MW m^{-2}), samples prepared in 45, 60, and 90 s show a more reasonable degree of browning while an exposure time of 36 s results in an increase in lightness after processing. During conventional bread baking, an increase in dough lightness tends to correspond to the first stage of baking (Purlis, 2010). The temperature and water activity of the food system conditions do not allow for browning reactions to occur. This same effect can be observed for the sample heated for 90 s at a beam flux of 0.32 MW m^{-2} and the samples laser-heated for 36, 45, and 60 s at a beam flux of 0.89 MW m^{-2} where an exposure time of 180 s still results in excessive browning; dough underneath the crust becomes visible due to clumping of the burnt material.

More optimal browning occurs at an exposure time of 90 s and energy flux of 0.89 MW m^{-2}. Samples processed for 36, 45, and 60 s with a beam flux of 0.50 and 0.32 MW m^{-2} show a negligible difference. These samples appear slightly darker than raw dough. Degree of browning in dough is very sensitive to beam flux; for an exposure time of 180 s, dough transition from very dark at 0.50 MW m^{-2} to a more conventional brown at 0.32 MW m^{-2}.

While optimal sample exposure time and beam flux for browning are limited, these variables can be tuned to achieve desired surface color for browning and crust development. Qualitative analyses by visual inspection and quantitative analyses by imaging surface color are important for assessing quality of baked dough (Yam & Papadakis, 2004). An approximate color range of 31–72 for *L*, 3–15 for *a*, and 15–33 for *b* can be used to determine satisfactory crust development (Shittu, Raji, & Sanni, 2007). Qualitatively, the most satisfactory browning in dough was achieved at a beam flux of 0.32 MW m^{-2} and exposure time of 180 s. Quantitatively, the mean surface color (L = 57.1, a = 7.8, b = 35.4) generated by these laser-heating parameters, however, narrowly misses the region of colors that would classify it as bread crust (*b* is slightly higher) (Mohd Jusoh, Chin, Yusof, & Rahman, 2009; Shittu et al., 2007); this variance can be accounted for with dough recipe and lighting conditions. Other laser fluxes that generated favorable browning results include 1) a flux of 2.03 MW m^{-2} at 45, 60, and 90 s exposure time; 2) a flux of 0.89 MW m^{-2} at 90 s exposure time; and 3) a flux of 0.5 MW m^{-2} at 90 s exposure time. Of these listed test cases, a flux of 2.03 MW m^{-2} at 60 and 90 s exposure time and a flux of 0.89 MW m^{-2} at 90 s exposure time yield *Lab* surface colors that match the quality of the outer crust of conventionally baked bread (Mohd Jusoh et al., 2009). Fig. 7 and Video 1 display the controlled progression of laser-induced browning.

3.2.2. Effect of beam power on dough browning

Changing the laser power while keeping the speed and beam diameter of the laser constant allows for tunable and controlled browning (Fig. 8). There are two ways to increase laser energy flux: 1) increase the spot size by increasing *z* or 2) increase the power of the laser. In the

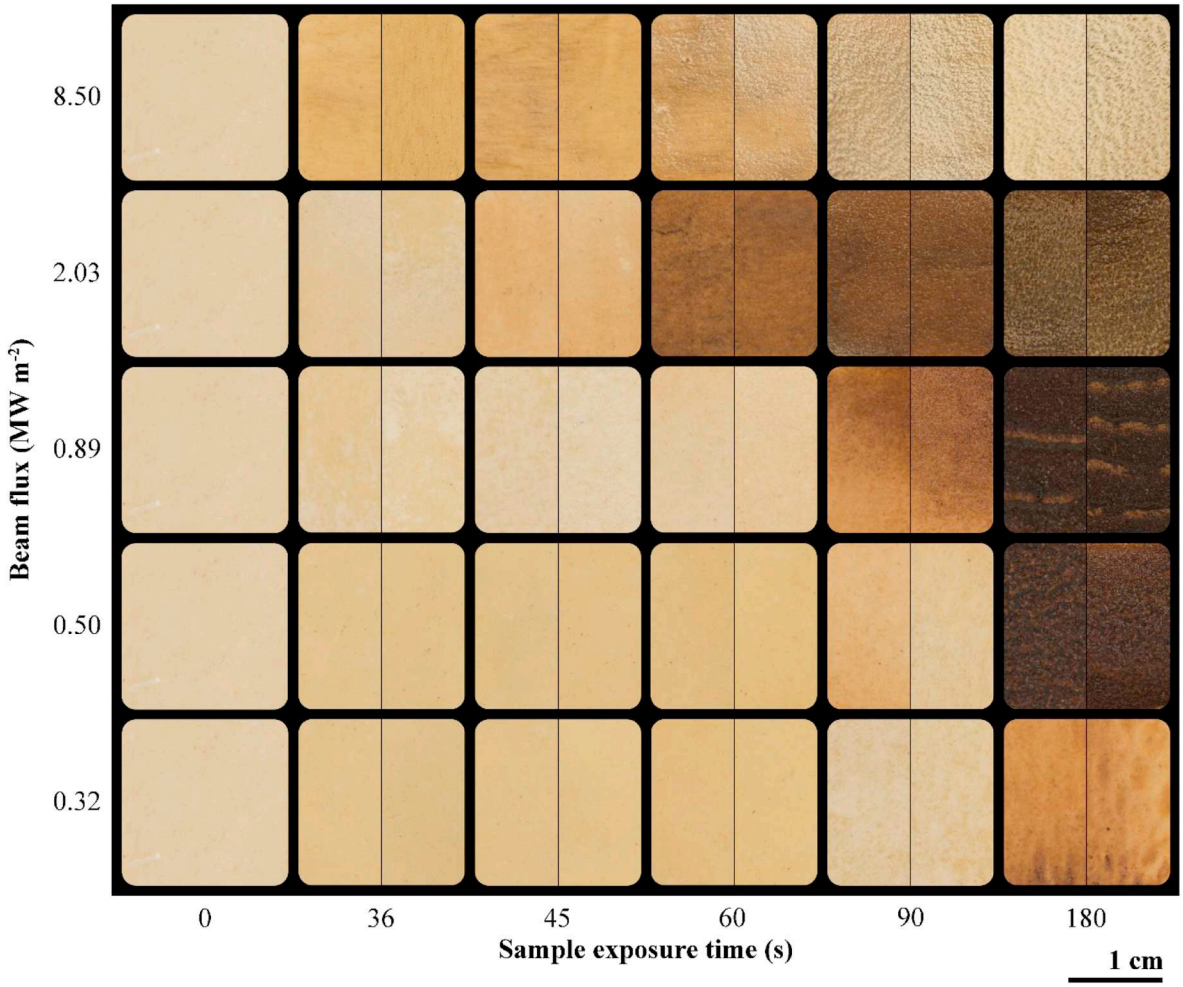

Fig. 6. Dough samples browned with a CO_2 laser. The raw dough sample is shown at an exposure time of 0 s. Duplicate tests were run for each of the heated samples; the left-hand portion of the tile is the first test and the right-hand portion is the second test. The tests were very repeatable.

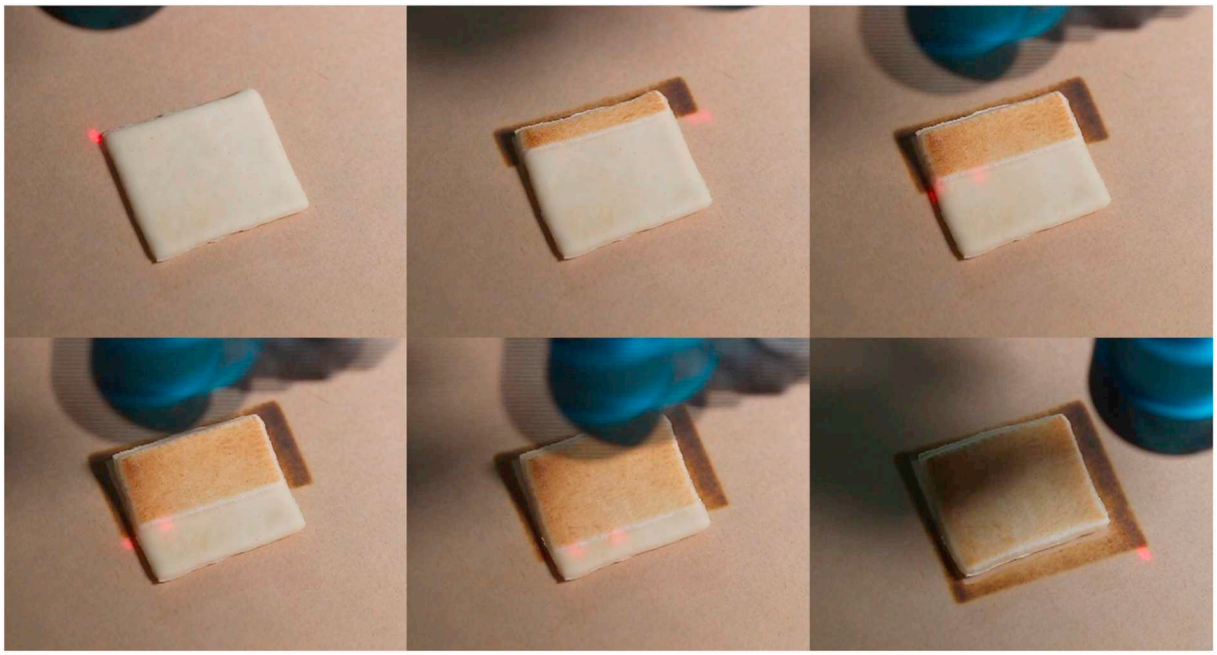

Fig. 7. Laser browning time-lapse of dough sample, where parameters lead to browning (power = 8 W, beam diameter = 4.5 mm, flux = 0.5 MW m^{-2}, sample exposure time = 90 s, speed = 100 mm s^{-1}). The laser head (blue) moves in an x-swing scanning pattern.

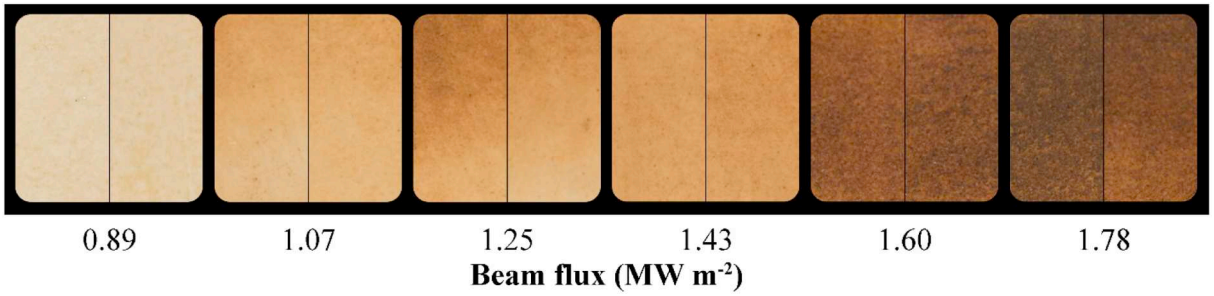

Fig. 8. Duplicate samples of dough baked with a CO_2 laser at increasing beam flux. The beam diameter (3.4 mm) and the sample exposure time (45 s, or speed of 200 mm s^{-1}) were kept constant during these tests. Beam power increases from left to right as follows: 8, 9.6, 11.2, 12.8, 14.4, and 16 W. Surface color progressively darkens as flux increases.

prior Section (3.2.1), the first method was used, while in this section the second method is explored. In these tests, the power of the laser is steadily increased at constant beam diameter, resulting in an increased energy flux. By increasing the amount of flux, and keeping other variables constant, the effect of increasing power can be observed. Increasing energy supplied clearly results in additional surface browning of the samples.

3.2.3. Predicting dough browning by symbolic regression

Understanding the effects of energy, beam flux, point exposure time, and variance of beam energy on the dough are essential for achieving controlled browning. As such, a symbolic regression was used to define a relationship among these variables. This genetic programming method is widely used in various domains for its efficacy (Koza, 2010), and involves searching a space of mathematical operations to find a model that fits a given dataset. Chen et al. (2019) has already modeled the laser-induced browning behavior of dough using a deep learning approach with a larger data set. Given the limited size and sparsity of this data set, the cross-validation technique that was employed provided the best results.

Browning will occur on the surface of a dough product when energy or flux is increased while other variables are constant (Fig. 8). Additionally, excessive energy or flux will yield to burning or vaporization of the dough (upper right corner of Fig. 6). Given the large set of variables that can affect the browning, a symbolic regression was used to develop a function that relates the energy per area (e, calculated from Eq. (2)), flux (f, calculated from Eq. (1)), point exposure time (p, calculated from Eq. (3)), and variance (v) to the lightness value (L) of a laser-browned dough sample. For each of the dough samples, L was determined by averaging the *Lab* value from a cluster of pixels taken from the center of each sample. L is used because it represents the most accurate indicator of surface color darkness.

The generative modeling software automatically split 90% of the data for training and 10% for validation with the responses taken from validation. The regression generated multiple equations that accurately predict a dough products level of browning.

$$\mathrm{L} = \boldsymbol{A_1} + \boldsymbol{B_1 v} + \boldsymbol{C_1 f} + \boldsymbol{D_1 E_1} \exp(\boldsymbol{F_1 v} - \boldsymbol{G_1}) \tag{5}$$

$$\boldsymbol{L} = \boldsymbol{A_2 e} + \boldsymbol{B_2 p^2} - \boldsymbol{C_2} + \boldsymbol{D_2 E_2} \exp(\boldsymbol{F_1 v} - \boldsymbol{G_1}) - \boldsymbol{H_2 p} - \boldsymbol{I_2 e^2} \tag{6}$$

$$\boldsymbol{L} = \boldsymbol{A_3 e} + \boldsymbol{B_3 p^2} - \boldsymbol{C_3} + \boldsymbol{D_3 E_3} \exp(\boldsymbol{F_1 v} - \boldsymbol{G_1}) - \boldsymbol{H_3 p} - \boldsymbol{I_3 e^2} + \frac{\boldsymbol{J_3} - \boldsymbol{K_3 f}}{\boldsymbol{v} - \boldsymbol{L_3}} \tag{7}$$

Of the 27 equations generated by the regression, three solutions (Eqs. (5), (6), and (7)) were selected because of their variance in complexity and goodness of fit (see Appendix A for non-symbolic form). There is an inherent tradeoff between complexity and accuracy that becomes apparent in the visualization of these equations in Fig. 9. For goodness of fit values > 0.84, each solution offers reliable approximations for calculating L. The ability to estimate the level of browning using only three variables further reinforces the degree of control achievable with a CO_2 laser in browning dough.

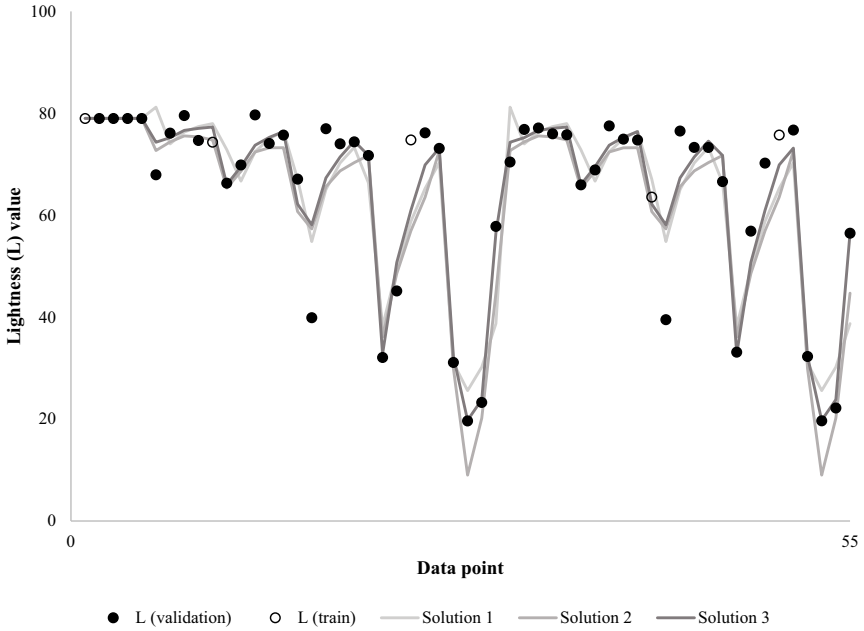

Fig. 9. Comparing the generative models (Solution 1, 2, and 3) to the data used to validate (L (validation)) and train (L (train)) the model. Solution 1 uses v and f as input variables; Solution 2 uses e, p, and v as input variables; Solution 3 uses e, p, v, and f as input variables. R^2 (goodness of fit) values for the solutions are 0.8499 for Solution 1, 0.9174 for Solution 2, and 0.9271 for Solution 3. The mean absolute errors as a percentage of maximum L are as follows: 6.54% for Solution 1, 4.36% for Solution 2, and 3.62% for Solution 3.

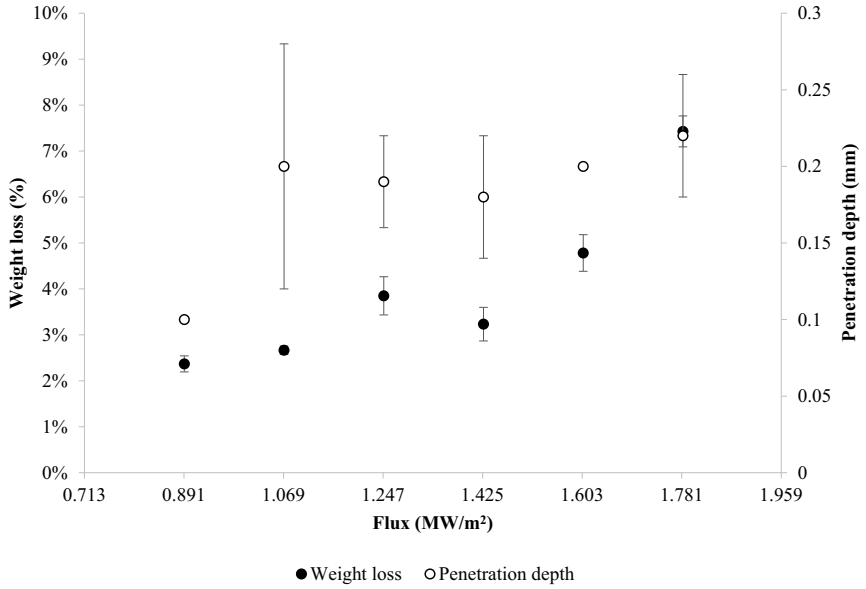

Fig. 10. Weight loss and penetration depth as a function of flux (beam diameter = 3.4 mm, sample exposure time = 45 s, speed = 200 mm s^{-1}). The error bars indicate standard error (SE) (n = 2). Weight loss increases with beam flux, while penetration depth was less conclusive.

3.2.4. Effect of laser flux on weight loss and thermal penetration depth

Similar to browning, weight loss is positively correlated to beam flux (Fig. 10); weight loss increases from 2.4% at 0.89 MW m^{-2} to 7.4% at 1.78 MW m^{-2}. Purlis and Salvadori (2007) also found a clear relationship between weight loss and brown color formation. The effect on thermal penetration depth was more difficult to measure because of the shallow penetration at these process parameters. Nonetheless, heat penetration depth increases from an average of 0.1 mm at 0.89 MW m^{-2} to 0.22 mm at a beam flux of 1.78 MW m^{-2} (Fig. 10). Increasing the amount of energy supplied increases moisture evaporation, brown color formation, and slightly increases heat penetration.

Amount of weight loss in the sample can be used to infer the amount of energy absorbed by the dough surface. As a control, an uncooked dough sample was exposed to ambient conditions and no change in weight was recorded over the course of 5 min, which exceeds the amount of time that a sample was exposed to the laser in a single test. One can, therefore, assume that change in weight is solely due to moisture evaporation from heating as opposed to ambient conditions. Fig. 11 shows the weight loss of the heated samples obtained by setting different laser beam fluxes for different exposure times.

At low exposure time, weight loss isn't very sensitive to beam diameter. This could be due to the fact that at a certain exposure time, total amount of energy applied remains the same. As exposure time is increased, however, beam diameter (i.e., energy flux) more greatly influences the weight loss. Weight loss reaches a maximum at highest energy flux—or smallest beam diameter—with a value of 24.8% (measured as a percent change from the pre-heated dough sample). Heat flux at small beam diameter is large enough to induce rapid moisture evaporation before conductive heat transfer can occur through the food. High energy flux also causes more moisture loss due to evaporation and dough powder to form. Due to high laser flux, moisture evaporation is so fast that dough completely dries out and transitions to powder before browning reactions can occur.

3.2.5. Effect of energy flux on thermal penetration depth in dough

Heat penetration inside the samples was measured at increasing exposure time and beam diameter (Fig. 12). As total laser energy supplied to the dough increases (directly proportional to exposure time), heat penetration depth increases (Fig. 12). At longer exposure times, laser flux more greatly affects thermal penetration. While weight loss reaches a maximum (24.8%) at the smallest beam diameter (1.1 mm), thermal penetration depth is highest (0.77 mm) at the largest tested beam diameter (5.7 mm). This can most likely be explained by thermal conduction. A larger beam diameter results in a lower laser heat flux,

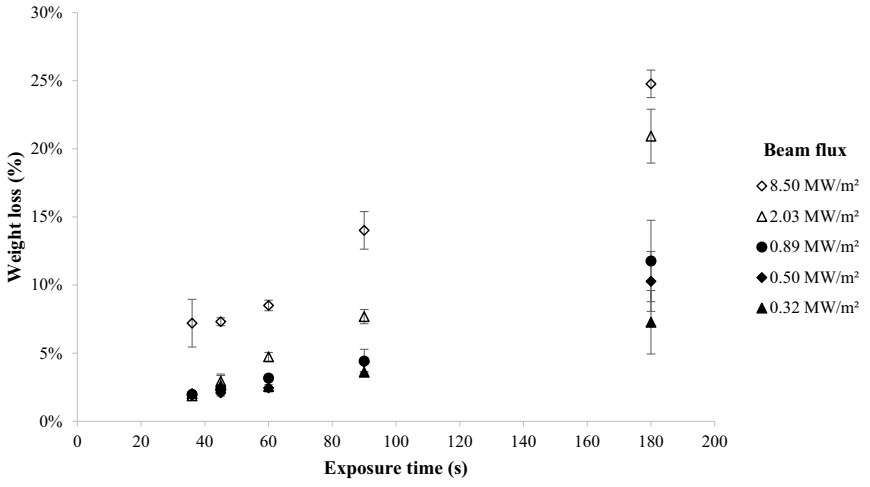

Fig. 11. Total weight loss of the dough samples obtained at different beam fluxes as a function of total exposure time. Low beam diameters correspond to high energy flux. Laser power remained constant at 8 W for these tests. The error bars indicate standard error (SE) (n = 2). There is a direct relationship between exposure time and weight loss.

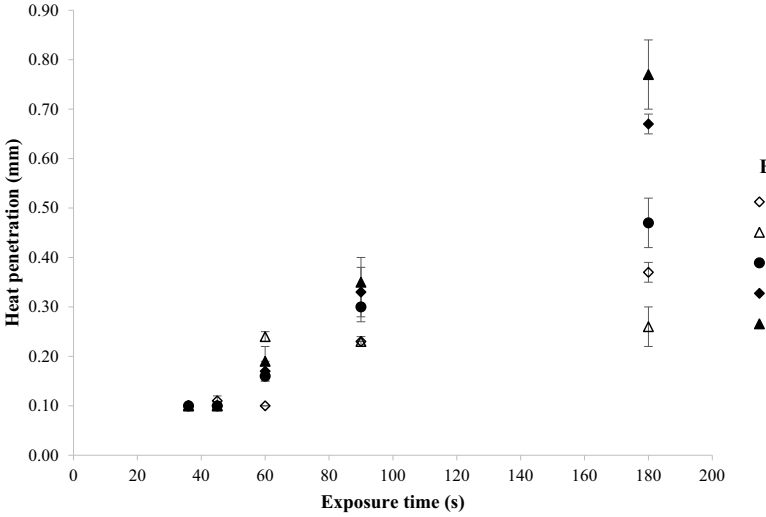

Fig. 12. Heat penetration depth in the dough samples obtained at different beam diameters as a function of total exposure time. Laser power remained constant at 8 W for these tests while beam diameter—therefore beam flux—was varied. The error bars indicate standard error (SE) (n = 2). There is a direct relationship between exposure time and weight loss.

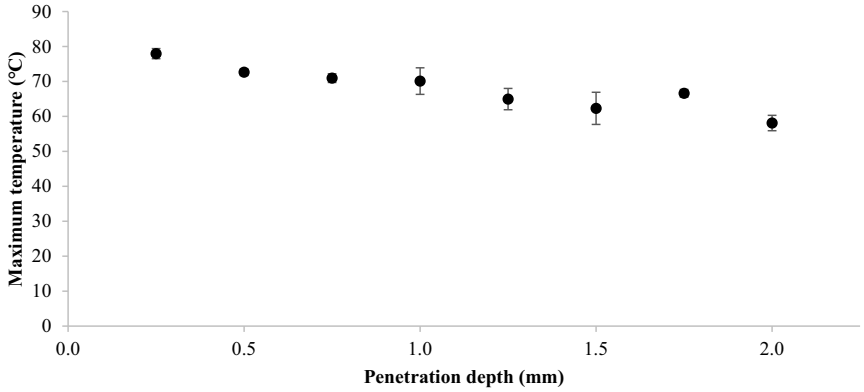

Fig. 13. Maximum temperatures inside the dough samples measured at increasing depth. The following laser parameters were held constant during these tests: beam diameter = 5.7 mm, exposure time = 180 s, and laser power = 8 W. The error bars indicate standard error (SE) (n = 2).

but the total amount of energy supplied to the food is constant. The interval between passes of the laser is fixed at 0.1 mm, therefore the material will be exposed to the laser during multiple passes. This results in a decrease in moisture evaporation and an increase in conductive heat transfer through the food, with time being the limiting factor in heat transfer. In brief, an increase in the penetration depth slows down the overall temperature increase of the food sample (Krishnamurthy et al., 2008), resulting in less moisture evaporation.

A linear regression was performed on the data to find a relationship between the different parameters. For the obtained results, heat penetration (h, mm) can be accurately estimated by the following formula, where t is the exposure time (s) and δ is the weight loss (g) (adjusted $R^2 = 0.90$):

$$\boldsymbol{h = 0.004441t - 0.75003\delta - 0.01932} \quad (8)$$

Beam diameter is accounted for in Eq. (8) since it plays an important role in weight loss by determining how much energy is transferred from the surface to the inside of the dough. At small beam diameters, weight loss is caused by moisture evaporation and material loss as well.

3.2.6. Effect of laser heating on internal dough temperature

Starch gelatinization is an important process that occurs only once certain temperatures are reached within the dough. Eight thermocouples were placed at 0.25 mm increments from the surface in order to measure the depth of heat penetration. A dough sample was exposed to the IR laser at a beam diameter of 5.7 mm for 180 s. Because the dough heating originates from the surface of the dough and relies on conductive heat transfer, maximum recorded temperatures decrease with increasing depth (Fig. 13), which is consistent with prior research (Blutinger et al., 2018).

Thermal penetration depth measured at these heating conditions was 0.77 mm. Temperatures less than a millimeter from the dough surface exceed 70 °C, which is just above the minimum temperature for initial swelling of starch granules (Olkku & Rha, 1978). Either the temperature was not maintained for sufficient time at deeper penetration depths for gelatinization to occur, or the temperatures reached were too low for gelatinization to take place. At a depth of 2 mm, the maximum temperature measured was 58 °C, which is too low to allow for starch gelatinization. Temperatures are not sufficient for complete starch gelatinization, which is required in bread crumb (Purlis, 2012). The minimum temperature should reach at least 95 °C to ensure complete gelatinization (Zanoni et al., 1995). Though full gelatinization was not achieved, SEM microscopy would allow for further microstructure analysis of the samples.

3.2.7. Comparing dough microstructure

Dough that has been heated via laser—as opposed to via oven—-develops different textural and visual properties (Fig. 14). The laser-browned dough product (beam diameter of 5.7 mm; sample exposure time of 180 s; laser power of 8 W) was compared to a sample prepared in a conventional hot air convection oven for 5 min—based on dough size and thickness—at 220 °C (heat setting for average baking application). With thin dough products, preparation in an oven will result in pillow-shaped dough expansion (right, Fig. 14). Blutinger et al. (2018) have already laser-baked dough with a blue laser and no significant expansion was observed, as is similar for the CO_2 laser-heated sample

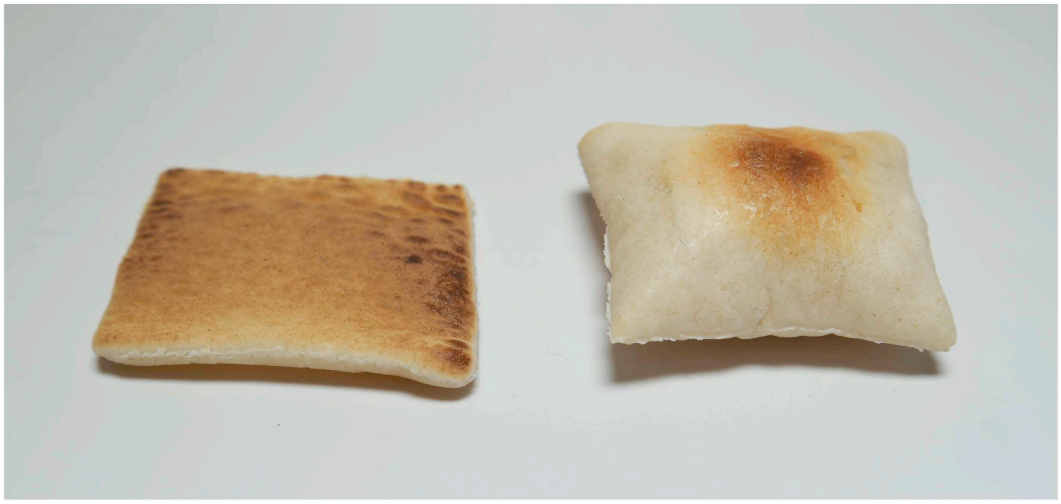

Fig. 14. Comparing a CO_2 laser-heated dough sample (left) to an oven-baked dough sample (right). Left: CO_2 laser-browned sample (beam diameter = 5.7 mm; sample exposure time = 180 s; laser power = 8 W); Right: oven-baked sample (220 °C for 5 min). The shape of the laser-heated sample remains the same while the oven-baked sample changes to a pillow-shape. Controlled browning is achieved in the laser-heated sample, while the oven-baked sample only browns at the center.

(left, Fig. 14). This is an advantage for FLM, where printed shape preservation is desired. Another disadvantage of preparing thin dough products in a convection oven is that the inside will be baked before sufficient browning can occur on the outside.

The transition of dough into crust and crumb can be examined by studying the microstructure by SEM. Gelatinization of starch can be used as an indication of the transition of dough into crumb. Fig. 15 presents a side view of the laser-browned dough sample, where the uncooked dough can be distinguished from the crumb by a difference in color. The darker portion underneath the dough crust was identified as crumb and analyzed by SEM.

SEM images can be used to check whether the starch granules are still intact (Almeida & Chang, 2013; Blutinger et al., 2018; Huang et al., 1990), because the granular form of starch is lost upon gelatinization (Ratnayake & Jackson, 2009). The microstructure of dough clearly consists of starch granules which are still intact. The variation in size is somewhere between 2 and 20 μm (A, Fig. 16), which corresponds to wheat starch granule sizes reported in literature (Olkku & Rha, 1978). Starch granules in the SEM image of the oven-baked sample (B, Fig. 16) show a dramatic size increase, which indicates starch swelling. This is in agreement with the results of Almeida and Chang (2013). Some of the smaller starch granules have lost their shape and become part of the network. The presence of air pockets in the structure is also evident, which occurred due to convective heating causing an expansion of the product. Conversely, the microstructure of the crumb of the CO_2 laser-heated sample (C, Fig. 16) shows starch granules that cannot be clearly distinguished. Granules appear to be swollen, disintegrated, and the microstructure is very tightly packed corresponding to the dough macrostructure. SEM images of CO_2 laser-browned dough also greatly differ from blue laser-baked dough (Blutinger et al., 2018) where starch

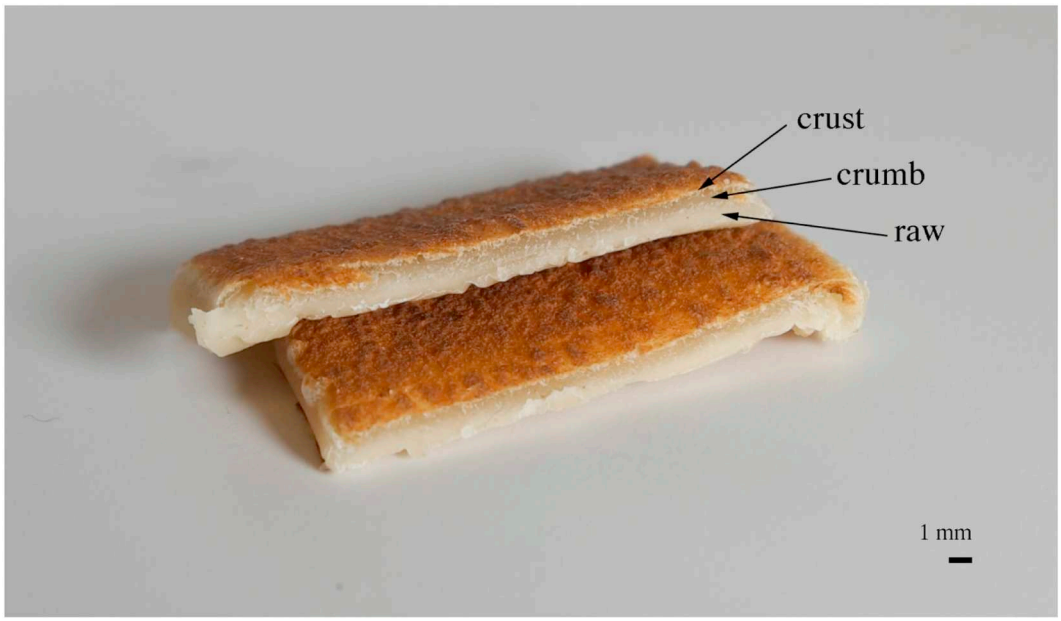

Fig. 15. Side view of a CO_2 laser-heated dough sample. Below the crust, the crumb can be observed, which is darker than the uncooked dough underneath it. The laser parameters for this test are as follows: beam diameter of 5.7 mm, sample exposure time of 180 s, laser power of 8 W.

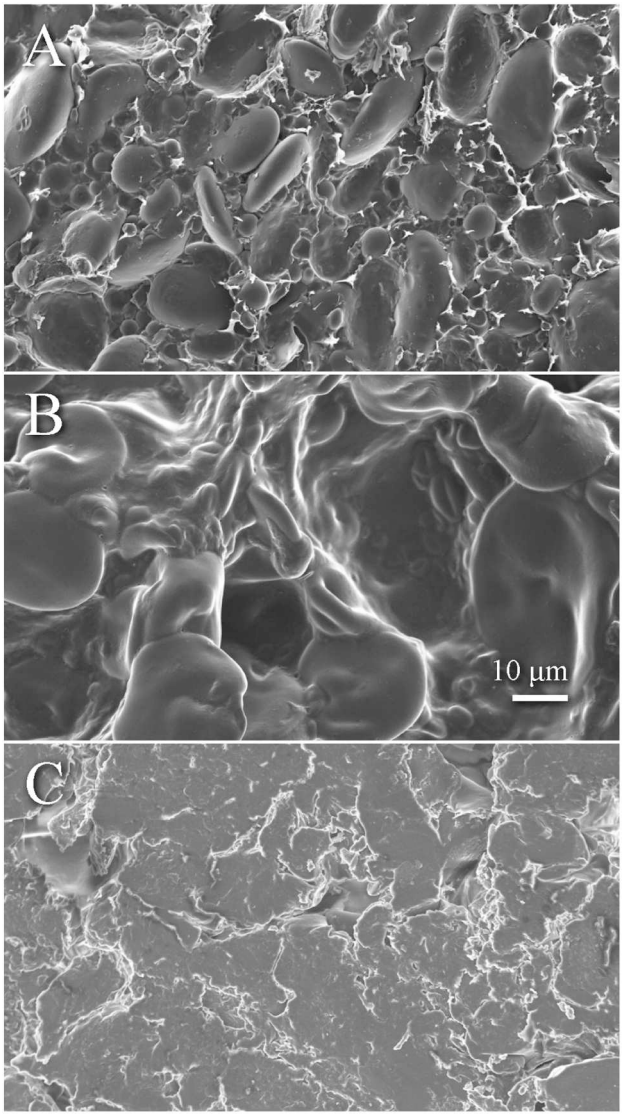

Fig. 16. Microstructure of various dough samples: A) raw uncooked, B) oven-baked, C) crumb of CO_2 laser-baked. Images were obtained in an SEM at 1000× magnification; scale bar shows 10 μm. Starch granules are intact in the raw dough sample (A) and significantly expanded in the oven baked sample (B). SEM image of the laser-browned sample (C) was taken from inside the heated dough sample.

granule swelling more closely resembles that of an oven-baked dough sample.

Microstructure of the CO_2 laser-heated sample was clearly different from a conventionally baked product. The expansion behavior of the product in the oven plays an important role. The images seem to indicate that the starch in the laser-browned sample has undergone structural change but full gelatinization of starch cannot be deduced from the SEM images.

4. Conclusions

Our study of the use of a CO_2 laser to effectively heat dough shows that the laser can brown the outer surface of dough products at a fast rate while maintaining spatial and thermal precision. The infrared wavelength of 10.6 μm results in high surface absorbance and—as a result—controlled degree of browning, better than conventional baking processes. When thermal penetration is required, however, laser flux should be decreased and exposure time increased for lower resolution to allow for more heat to propagate through the dough by conduction. The highest heat penetration achieved for our CO_2 laser was 0.77 mm. Tandem use of a CO_2 laser and a blue laser provide the ability to accurately localize heat, thermally penetrate food, and maintain the shape of the pre-cooked food making them optimal for more personalized nutrition in 3D food printing applications, sheet-dough products, and custom browning applications in processed meat production.

Supplementary data to this article can be found online at https://doi.org/10.1016/j.ifset.2018.11.013.

Acknowledgements

This work was supported in part by Columbia University's SEAS Interdisciplinary Research Seed (SIRS) funding program.

Appendix A

Full solutions from symbolic regression:

All of the data was normalized, prior to feeding it into the generative model, by means of subtracting the average of each data set and dividing by the standard deviation. Large coefficients are a result of very small values for the variance of energy supplied to the dough sample ($\boldsymbol{v}$).

Solution 1:

$$L = 18 + 7.371 \times 10^{10}v + 5.589f + 4.732 \times 0.001674^{(7.371\times10^{10}v-0.4)}$$

$R^2 = 0.8499$, $MAE = 5.2096(6.54\%)$.

Solution 2:

$$L = 0.206e + 1.309p^2 - 33.54 + 26.03 \times 0.02573^{(7.371\times10^{10}v-0.4)} - 2.402p - 8.933 \times 10^{-5}e^2$$

$R^2 = 0.9174$, $MAE = 3.4772(4.36\%)$.

Solution 3:

$$L = 0.2039e + 1.32p^2 - 33.18 + 27.79 \times 0.02942^{(7.371\times10^{10}v-0.4)} - 2.422p - 8.807 \times 10^{-5}e^2 + \frac{9.133 \times 10^{-12} - 9.559 \times 10^{-13}f}{v - 5.426 \times 10^{-12}}$$

$R^2 = 0.9271$, $MAE = 2.8825(3.62\%)$.

References

Abdullah, M. Z. (2008). 20 – Quality evaluation of bakery products. *Computer vision technology for food quality evaluation* (pp. 481–522). .

Ahrné, L., et al. (2007). Effect of crust temperature and water content on acrylamide formation during baking of white bread: Steam and falling temperature baking. *LWT - Food Science and Technology, 40*(10), 1708–1715.

Almeida, E. L., & Chang, Y. K. (2013). Structural changes in the dough during the pre-baking and re-baking of French bread made with whole wheat flour. *Food and Bioprocess Technology, 6*(10), 2808–2819.

Baranov, G. A., et al. (2005). Modification of biological objects in water media by CO2 laser radiation. *Quantum Electronics, 35*(9), 867–872.

Blutinger, J. D., et al. (2018). Characterization of dough baked via blue laser. *Journal of Food Engineering, 232*, 56–64. http://linkinghub.elsevier.com/retrieve/pii/S026087741830133X (April 3, 2018).

Chen, P. Y., et al. (2019). Visual modeling of laser-induced dough browning. *Journal of Food Engineering, 243*, 9–21. https://www.sciencedirect.com/science/article/pii/S0260877418303595 (September 11, 2018).

Datta, A. K., & Rakesh, V. (2013). Principles of microwave combination heating. *Comprehensive Reviews in Food Science and Food Safety, 12*(1), 24–39. http://doi.wiley.com/10.1111/j.1541-4337.2012.00211.x (September 27, 2018).

Dessev, T., Jury, V., & Le-Bail, A. (2011). The effect of moisture content on short infrared absorptivity of bread dough. *Journal of Food Engineering, 104*(4), 571–576.

Diaz, J. V., et al. (2014). *Method for the production of edible objects using SLS and food products WO 2014193226 A1*.

Fukuchi, K., Jo, K., Tomiyama, A., & Takao, S. (2012). Laser cooking. *Proceedings of the ACM multimedia 2012 workshop on multimedia for cooking and eating activities - CEA '12* (pp. 55). New York, New York, USA: ACM Press.

Gordon, E. I. (2000). Use of lasers in ophthalmic surgery. *IEEE Journal of Selected Topics in Quantum Electronics, 6*(6), 1116–1121. http://ieeexplore.ieee.org/document/902160/ (October 18, 2017).

Gracia, A., & Sepulveda, E. (2015). *Apparatus and method for heating and cooking food using laser beams and electromagnetic radiation WO 2016053681 A1*.

Griesbach, L.,. et al. Method of providing grill marks on a foodstuff. (2004). https://patents.google.com/patent/US20050008742A1/en (July 26, 2018).

Hertafeld, E., Zhang, C., Jin, Z., Jakub, A., Russell, K., Lakehal, Y., ... Lipson, H. (2018). Multi-material three-dimensional food printing with simultaneous infrared cooking. *3D Printing and Additive Manufacturing: 3dp* (pp. 0042). . (November 28, 2018) https://www.liebertpub.com/doi/10.1089/3dp.2018.0042.

Huang, J., et al. (1990). Scanning electron microscopy: tissue characteristics and starch granule variations of potatoes after microwave and conductive heating. *Food Structure, 9*(9), 113–122. http://digitalcommons.usu.edu/foodmicrostructure (February 3, 2018).

Kaplan, A. (1994). A model of deep penetration laser welding based on calculation of the keyhole profile. *Journal of Physics D: Applied Physics, 27*(9), 1805–1814. http://stacks.iop.org/0022-3727/27/i=9/a=002?key=crossref.03f7e3ef991bd0b56cbc882399ebf226 (October 18, 2017).

Koza, J. R. (2010). Human-competitive results produced by genetic programming. *Genetic Programming and Evolvable Machines, 11*(3–4), 251–284. http://link.springer.com/10.1007/s10710-010-9112-3 (October 20, 2017).

Krishnamurthy, K., et al. (2008). Infrared heating in food processing: An overview. *Comprehensive Reviews in Food Science and Food Safety, 7*(1), 2–13.

Lentz, R. R., et al. (1995). *Method of processing food utilizing infrared radiation US 5382441 A*.

Lineback, D. R., & Wongsrikasem, E. (1980). Gelatinization of starch in baked products. *Journal of Food Science, 45*(1), 71–74.

Lipson, H., & Kurman, M.. Fabricated: The new world of 3D printing. (2013). https://books.google.com/books?hl=en&lr=&id=MpLXWHp-srIC&oi=fnd&pg=PA1&dq=3d+food+printing&ots=Z3bZySJ3_H&sig=J0B9KCDystLtS9v1aa-Ub2wECzg#v=onepage&q=3d+food+printing&f=false (May 27, 2018).

Miller, B. S., Derby, R. I., & Trimbo, H. B. (1973). A pictorial explanation for the increase in viscosity of a heated wheat starch-water suspension. *Cereal Chemistry, 50*, 271–280.

Mohd Jusoh, Y. M., Chin, N. L., Yusof, Y. A., & Rahman, R. A. (2009). Bread crust thickness measurement using digital imaging and L a b colour system. *Journal of Food Engineering, 94*(3–4), 366–371. https://www.sciencedirect.com/science/article/pii/S0260877409001885 (October 25, 2018).

Mondal, A., & Datta, A. K. (2008). Bread baking – A review. *Journal of Food Engineering, 86*(4), 465–474.

Muchnik, B. (2008). *Laser cooking apparatus US 20080282901 A1*.

Olkku, J., & Rha, C. K. (1978). Gelatinisation of starch and wheat flour starch—A review. *Food Chemistry, 3*(4), 293–317.

Panchev, I. N., Kirtchev, N. A., & Dimitrov, D. D. (2011). Possibilities for application of laser ablation in food technologies. *Innovative Food Science & Emerging Technologies, 12*(3), 369–374.

Periard, D., et al. (2007). Printing food. *Proceedings of the 18th Solid Freeform Fabrication Symposium, Austin, TX* (pp. 564–574). . https://sffsymposium.engr.utexas.edu/Manuscripts/2007/2007-48-Periard.pdf (November 30, 2017).

Ploteau, J. P., Glouannec, P., Nicolas, V., & Magueresse, A. (2015). Experimental investigation of French bread baking under conventional conditions or short infrared emitters. *Applied Thermal Engineering, 75*, 461–467.

Purlis, E. (2010). Browning development in bakery products – A review. *Journal of Food Engineering, 99*(3), 239–249.

Purlis, E. (2012). Baking process design. *Handbook of food process design* (pp. 743–768). Oxford, UK: Wiley-Blackwell.

Purlis, E., & Salvadori, V. O. (2007). Bread browning kinetics during baking. *Journal of Food Engineering, 80*(4), 1107–1115.

Rastogi, N. K. (2015). 5 – Infrared heating of foods and its combination with electron beam processing. *Electron beam pasteurization and complementary food processing technologies* (pp. 61–82). .

Ratnayake, W. S., & Jackson, D. S. (2009). Starch gelatinization. *Advances in Food and Nutrition Research, 55*, 221–268.

Salagnac, P., Glouannec, P., & Lecharpentier, D. (2004). Numerical modeling of heat and mass transfer in porous medium during combined hot air, infrared and microwaves drying. *International Journal of Heat and Mass Transfer, 47*(19), 4479–4489.

Shittu, T. A., Raji, A. O., & Sanni, L. O. (2007). Bread from composite cassava-wheat flour: I. Effect of baking time and temperature on some physical properties of bread loaf. *Food Research International, 40*(2), 280–290. https://www.sciencedirect.com/science/article/pii/S0963996906001815 (October 25, 2018).

Singh, I. (2013). *Method and apparatus for plasma assisted laser cooking of food products US 2013/0344208 A1*. 14.

Skjöldebrand, C., & Andersson, C. (1989). A comparison of infrared bread baking and conventional baking. *Journal of Microwave Power and Electromagnetic Energy, 24*(2), 91–101.

Steen, W. M., & Mazumder, J. (2010). *Laser material processing* (4th ed.). Springer.

Sun, J., et al. (2015). An overview of 3D printing technologies for food fabrication. *Food and Bioprocess Technology, 8*(8), 1605–1615. http://link.springer.com/10.1007/s11947-015-1528-6 (May 27, 2018).

Wang, S., & Copeland, L. (2013). Molecular disassembly of starch granules during

gelatinization and its effect on starch digestibility: A review. *Food & Function, 4*(11), 1564.

Wegrzyn, T. F., Golding, M., & Archer, R. H. (2012). Food layered manufacture: A new process for constructing solid foods. *Trends in Food Science & Technology, 27*(2), 66–72. https://www.sciencedirect.com/science/article/pii/S0924224412000921 (April 24, 2018).

Westerberg, E. R. (1998). *Apparatus and method for cooking food with a controlled spectrum US 6069345 A*.

Wheeland, R. G. (1995). Clinical uses of lasers in dermatology. *Lasers in Surgery and Medicine, 16*(1), 2–23. http://doi.wiley.com/10.1002/lsm.1900160103 (October 18, 2017).

Yam, K. L., & Papadakis, S. E. (2004). A simple digital imaging method for measuring and analyzing color of food surfaces. *Journal of Food Engineering, 61*(1), 137–142. https://www.sciencedirect.com/science/article/pii/S026087740300195X (October 25, 2018).

Zanoni, B., Peri, C., & Bruno, D. (1995). Modelling of browning kinetics of bread crust during baking. *LWT - Food Science and Technology, 28*(6), 604–609.

Zoran, A., & Coelho, M. (2011). *Cornucopia: The concept of digital gastronomy. 44(5)*, MIT Press425–431. http://muse.jhu.edu/journals/len/summary/v044/44.5.zoran.html (December 5, 2017).